AGU PUBLICATIONS

Water Resources Research

RESEARCH ARTICLE
10.1002/2017WR021585

Nine Hundred Years of Weekly Streamflows: Stochastic Downscaling of Ensemble Tree-Ring Reconstructions

David Sauchyn[1] **and Nesa Ilich**[2]

[1]Department of Geography and Environmental Studies, University of Regina, Regina, SK, Canada, [2]Optimal Solutions Ltd., Calgary, AB, Canada

Key Points:
- We combined the methods and advantages of paleo and stochastic hydrology to estimate 900 years of weekly flows for two major rivers in Alberta, Canada
- We developed a new algorithm to generate stochastic time series of weekly flows that have decadal variability not evident in the short historical flow record
- A second innovation is to derive the paleohydrology from an ensemble of 100 statistically significant reconstructions at each gauge

Supporting Information:
- Supporting Information S1

Correspondence to:
D. Sauchyn,
sauchyn@uregina.ca

Citation:
Sauchyn, D., & Ilich, N. (2017). Nine hundred years of weekly streamflows: Stochastic downscaling of ensemble tree-ring reconstructions. *Water Resources Research*, *53*. https://doi.org/10.1002/2017WR021585

Received 21 JUL 2017
Accepted 11 OCT 2017
Accepted article online 16 OCT 2017

Abstract We combined the methods and advantages of stochastic hydrology and paleohydrology to estimate 900 years of weekly flows for the North and South Saskatchewan Rivers at Edmonton and Medicine Hat, Alberta, respectively. Regression models of water-year streamflow were constructed using historical naturalized flow data and a pool of 196 tree-ring (earlywood, latewood, and annual) ring-width chronologies from 76 sites. The tree-ring models accounted for up to 80% of the interannual variability in historical naturalized flows. We developed a new algorithm for generating stochastic time series of weekly flows constrained by the statistical properties of both the historical record and proxy streamflow data, and by the necessary condition that weekly flows correlate between the end of a year and the start of the next. A second innovation, enabled by the density of our tree-ring network, is to derive the paleohydrology from an ensemble of 100 statistically significant reconstructions at each gauge. Using paleoclimatic data to generate long series of weekly flow estimates augments the short historical record with an expanded range of hydrologic variability, including sequences of wet and dry years of greater length and severity. This unique hydrometric time series will enable evaluation of the reliability of current water supply and management systems given the range of hydroclimatic variability and extremes contained in the stochastic paleohydrology. It also could inform evaluation of the uncertainty in climate model projections, given that internal hydroclimatic variability is the dominant source of uncertainty.

1. Introduction

The design and management of infrastructure for the storage, allocation, and conveyance of water is based almost exclusively on the analysis of instrumental weather and water records, which usually are limited in length to less than 100 years, and in many basins to less than 50 years. This record length is insufficient for supporting planned adaptation to climate change, especially if the range of water levels is amplified by global warming as projected (Durack et al., 2012; Kharin et al., 2007). Model projections of future hydroclimate are subject to three main sources of uncertainty. Two of them, differences among climate models and greenhouse gas emission scenarios, become increasingly relevant in distal decades as the models simulate escalating anthropogenic forcing; however, for proximal decades the internal variability of the climate system is the dominant source of uncertainty (Deser et al., 2014; Knutti & Sedláček, 2012). Biological and geological proxies are the only empirical source of data on the range of natural variability that includes both historically negligible, and recently more significant, human intervention in global climate and regional ecosystems.

Tree rings are a source of hydroclimatic data, and an absolute annual chronology, for the time intervals spanned by living trees and cross-dateable dead wood. Streamflow is the hydrologic variable most often reconstructed from tree rings using the methods and principles of dendrohydrology (Meko & Woodhouse, 2011). The annual growth increment and water balance data often correlate. Seasonal reconstructions of hydrologic variables have been derived from the properties of latewood and earlywood (Meko & Baisan, 2001; Meko et al., 2013). Ring-width data from long-lived trees growing at dry sites is an effective proxy of seasonal and annual water levels, because (1) the growth of these trees is limited by the availability of soil moisture and thus the same weather variables (precipitation, temperature, evapotranspiration) that determine river flow also control tree growth, and (2) there is a similar integrating and lagged response of tree growth and streamflow to inputs of precipitation. This shared response of radial tree growth and runoff to the near surface water balance is the basis for the reconstruction of streamflow from standardized ring-width data (Elshorbagy et al., 2016; Loaiciga et al., 1993).

The principles of dendrohydrology are sufficiently well established that, in some river basins, streamflow reconstructions have been applied to water resource management (Meko & Woodhouse, 2011; Sauchyn et al., 2015a, 2015b). However, despite the superior resolution of tree rings relative to other climate proxies, water resource engineering and management usually require hydrometric data of weekly, or at least seasonal, resolution. In this paper, we address this limitation with a novel research design that combines the advantages of paleo and stochastic hydrology. We devised a new algorithm to reconstruct multicentury streamflow time series with weekly resolution, capturing both the seasonal variability in recorded streamflow and the interannual to decadal variability in the tree-ring record. The basic premise is that a synthetic time series of weekly flows can be generated to satisfy the weekly statistics of natural flows derived from the available historical record, while simultaneously conforming to the annual hydrologic sequences inferred from tree rings. To the best of our knowledge, there has been no previous attempt to estimate weekly natural flows based on the statistical properties of tree-ring and gauged streamflow data. This approach has the potential to yield centuries of high-resolution proxy hydrometric data.

Stochastic hydrology has been an active area of research since the early 1970s, evolving in the last three decades as a special branch of the earth sciences that combines hydrology and statistical methods for the purpose of generating randomized times series that can closely represent natural hydrologic processes. The use of stochastic time series as alternative inputs includes the evaluation of reservoir operating rules, drought management, water quality studies, and the design of hydraulic structures (Ilich, 2014; Ilich & Despotovic, 2008). Recent applications in Alberta (Canada) include real-time reservoir operating rules (Ilich, 2011), optimizing river basin allocation (Ilich, 2008), and river basin management (Ilich et al., 2000). Stochastic hydrology provides hydrologic variability that is statistically likely to occur, but also more challenging to manage than historical flows, either in terms of the magnitude of individual events or their duration, as in the case of consecutive dry years. A major shortcoming of stochastic hydrology, however, is that the generated output series preserve the annual flow statistics (means, variance, and autocorrelation) of relatively short instrumental records. Using proxy data to generate centuries of weekly flow estimates introduces hydrologic variability, and sequences of wet and dry years, that are not evident in the short historical flow record.

The objective of this project was to provide water management agencies and a private utility in Alberta (Canada) with robust tree-ring reconstructions of river flow for the assessment of water conveyance, storage, and treatment infrastructure and protocols under extreme hydroclimatic conditions. This objective was achieved using multiple tree-ring proxies across a dense network of 76 sites, and two methodological innovations introduced in this paper: (1) deriving the paleohydrology from an ensemble of statistically significant reconstructions at each gauge, and (2) stochastically downscaling the proxy water-year flows to weekly estimates. We develop and demonstrate this approach to applied paleohydrology using the Saskatchewan River Basin as a case study. We derive 100 member ensemble reconstructions and 900 years of weekly flows for two gauges: The North Saskatchewan River (NSR) at Edmonton and the South Saskatchewan River (SSR) at Medicine Hat (Figure 1).

2. The Case Study Watershed and Data

In the five states and two provinces that comprise the semiarid Northern Great Plains, urban settlement, and an industrial economy are enabled by runoff from the Rocky Mountains, although population density is relatively low and urban centers are relatively small, with the exception of southern Alberta. Most of the oil production and irrigated land in Canada is in Alberta. Nearly all of this industrial activity, and the major population centers, including Canada's third and fourth largest urban populations in Calgary and Edmonton, are confined to the North and South Saskatchewan River Basins (NSRB, SSRB; Figure 1). Whereas these two river basins are hydrologically similar, the use and demand for water differs, with irrigation accounting for most of the consumptive use of water in the SSRB and industrial activity, related to energy and oil production, dominating water demand in the NSRB (Government of Alberta, 2010).

The flow of the North and South Saskatchewan Rivers has been gauged since 1912 at Edmonton and Medicine Hat, respectively. Above these gauges, water is impounded in several reservoirs for the purposes of generating hydroelectricity and additionally, in the SSRB, for storing irrigation water. Therefore, we used naturalized weekly flows to construct tree-ring models and for scaling the annual proxy data to estimate

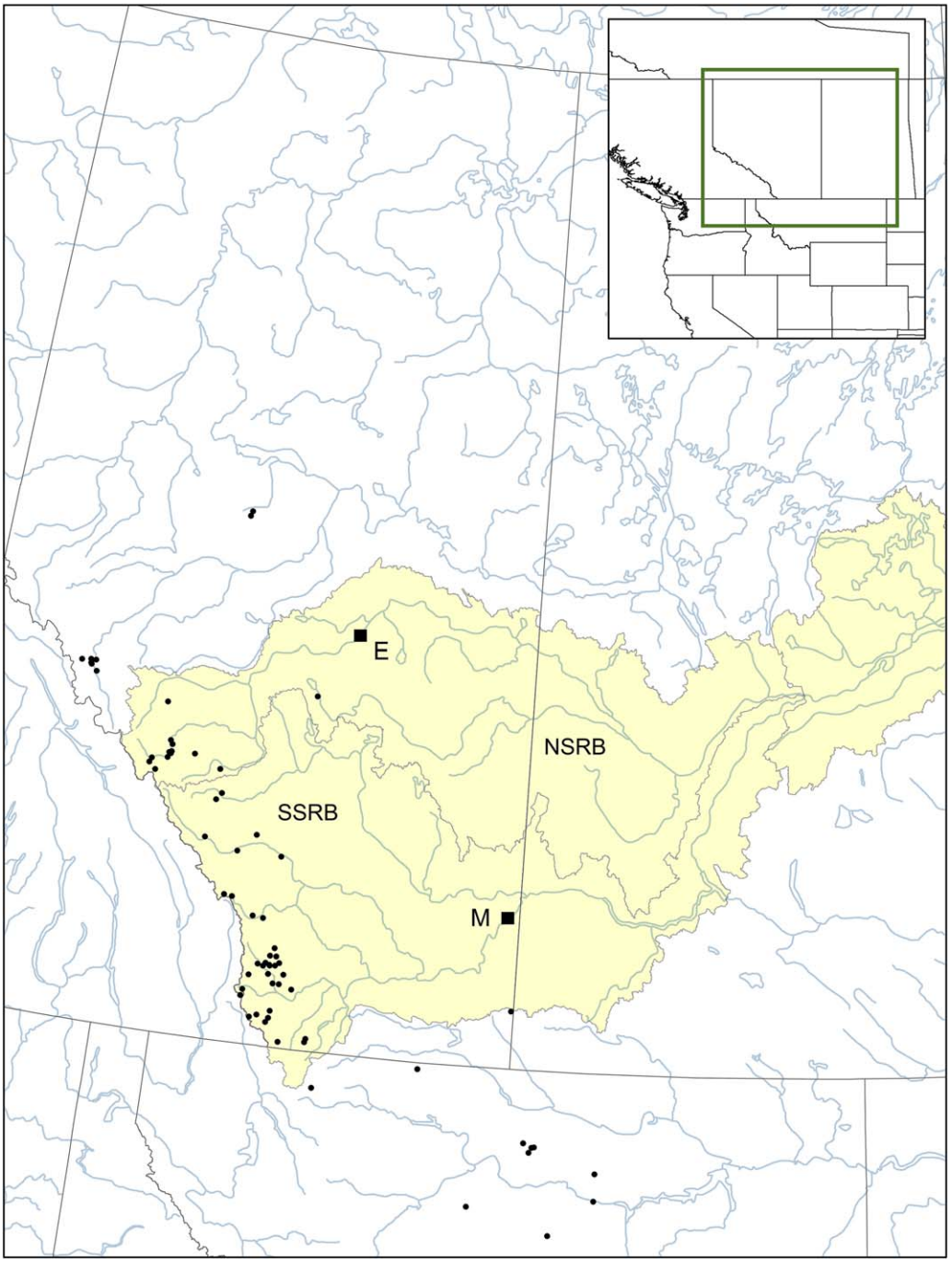

Figure 1. The North and South Saskatchewan River Basins (NSRB, SSRB) in Alberta and western Saskatchewan. The dots give the locations of our 76 tree-ring chronology sites located in the SSRB and NSRB and in adjacent river basins. Tree-ring data from these sites were used to reconstruct the flow of the North Saskatchewan River at Edmonton (E) and the South Saskatchewan River at Medicine Hat (M). The inset map shows the location of the study area relative to the states, provinces and territories of west-central North America.

weekly flow. The provincial water management agency has generated naturalized flow data using the project depletion method (i.e., recorded flows adjusted to account for the effects of storage and diversions). The procedure sums all adjustments on a daily basis for multiple locations in a river basin. Some abstractions are known; others are estimated. Storage change is calculated from recorded reservoir levels and outflows. Net reservoir evaporation is estimated. The procedure starts from the most upstream locations where it adjusts

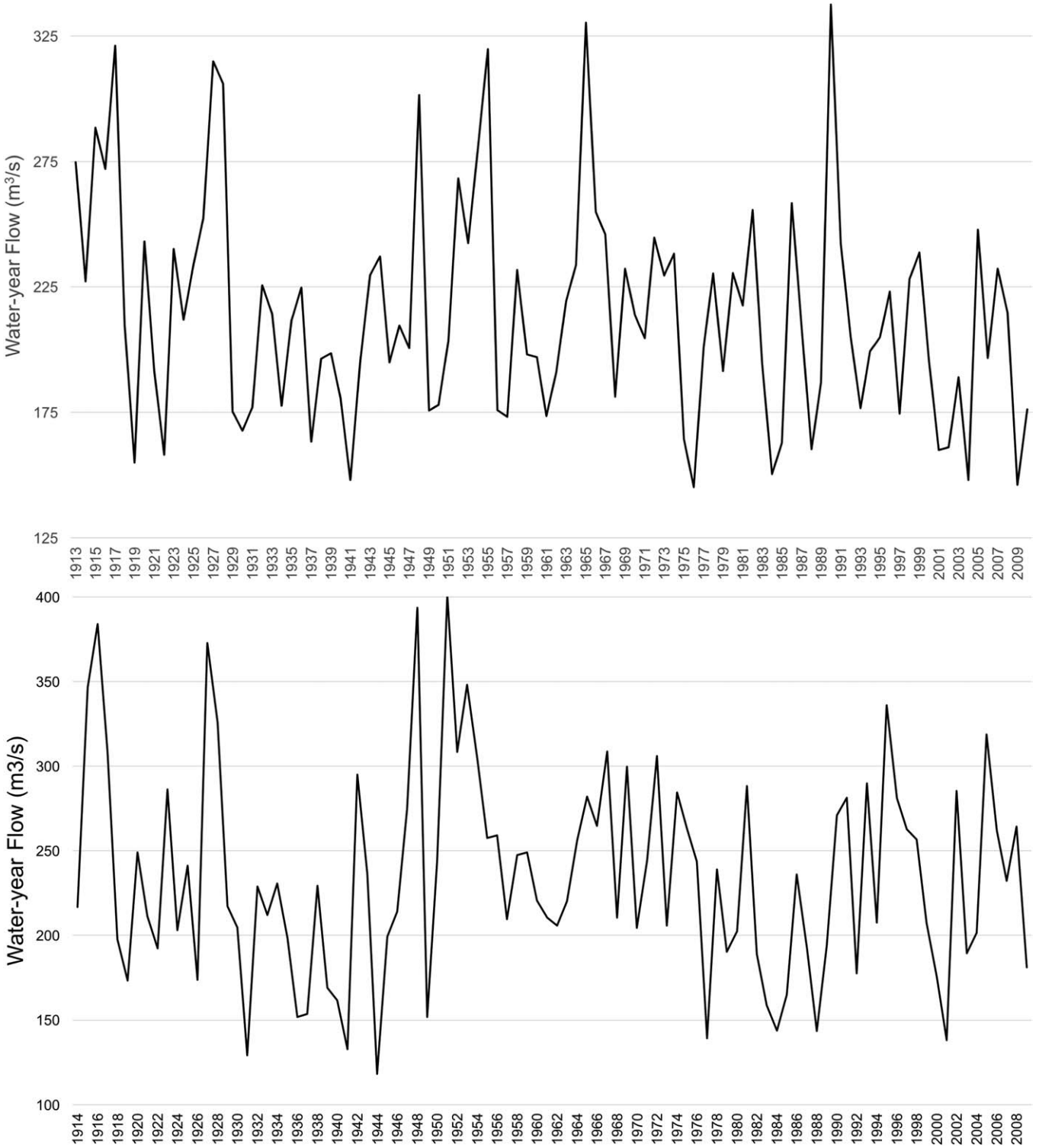

Figure 2. (top) The mean annual naturalized flow of the North Saskatchewan River at Edmonton, 1913–2010 and (bottom) the South Saskatchewan River at Medicine Hat, 1914–2009.

the flows for abstractions and storage change, including net evaporation on the incremental areas for lakes that have been raised from their natural levels by erected structures, or the total area if lakes have been created by dams at locations where they previously did not exist. The final step is the hydrologic routing of daily natural flows to a downstream point on each reach, and the adjustments are added to the routed flows. Time

series of naturalized water-year (October–September) flow for the two gauges (Figure 2) clearly show interannual and decadal modes of variability, which have been linked to the influence of the El Niño South Oscillation (ENSO) and Pacific Decadal Oscillation (PDO) on the hydroclimate of western North America (Sauchyn et al., 2015b, 2017). The decadal scale variability in particular warrants the longer view taken in this study. The mean monthly hydrograph of these rivers (not shown) is characteristic of midlatitude mountain watersheds with a nival hydrologic regime. Nearly 40% of the annual discharge occurs in June and July with the melt of the high-elevation snowpack, and relatively high flows are maintained through August from glacier meltwater runoff.

Studies of the dendrohydrology of mountainous river basins typically are based on tree-ring data from headwater subbasins, where most of the runoff is produced, and from adjacent watersheds since climate is not confined by drainage divides. Tree-ring data from the adjacent Missouri and Peace-Athabasca River basins are relevant here, and in fact correlate with gauged flows in the SRB. Therefore, our tree-ring network is composed of 76 sites (Figure 1), including seven sites where we augmented tree-ring data previously collected by other researchers, in particular, from Western University (Watson & Luckman, 2005). At each site, we collected cross sections of wood from dead trees and two increment cores per tree from living trees. In addition to annual ring-width, we measured the earlywood and latewood growth increments at most sites, producing a total 196 ring-width chronologies. The effort to establish an extensive tree-ring network, and collect a large amount of subannual ring-width data, is justified by the potential to capture more seasonal and spatial hydrometric variability than from annual ring-width data from a few sites, the approach taken by most previous studies in dendrohydrology. Geographic and statistical data for the tree-ring sites and chronologies are given in the supporting information Tables S1 and S2. The site chronologies range in length from 251 to 1463 years, exceeding 400 years at most of the sites. Laboratory methods for constructing the ring-width index chronologies are described in the supporting information.

3. Streamflow Reconstruction

For the purpose of blending paleo and stochastic hydrology, and generating nine millennia of weekly flows, we developed new reconstructions of the water-year (October–September) flow of the SSR at Medicine Hat and the NSR at Edmonton. Two previously published reconstructions of each river were based on tree-ring data from two and 14 sites for the SSR, and from two and seven sites for the NSR (Axelson et al., 2009; Case & Macdonald 2003; Sauchyn et al., 2011). Also, these previous studies used only a single annual ring-width chronology from each site, and thus a pool of between two and 14 tree-ring chronologies for the reconstruction of streamflow. From our pool of 196 tree-ring chronologies from 76 sites, 135 and 126 are significantly ($p < 0.05$) correlated with the naturalized water-year flow of the SSR and NSR, respectively. Thus, we were able to take advantage of substantially more, and more recent, tree-ring data and updated hydrometric records, and thereby produce robust reconstructions of the water-year flow of the NSR and SSR for the period 1110– 2010. We constructed tree-ring models of water-year (September–October) streamflow using standard methods in dendrohydrology (Meko et al., 2012). Stepwise forward regression was applied to groups (pools) of fewer but longer tree-ring chronologies generating a series of nested reconstructions for each river. These methods, including the calibration and verification procedures, are described in the supporting information. For each nested tree-ring model, the number of predictor chronologies was fixed at five to nine as a function of the size of the pool of potential predictors and incremental changes in the validation statistics with additional predictors.

Standard practice in dendrohydrology is to derive a single best reconstruction from a pool of potential predictor proxies of the regional hydroclimate. This conventional approach has evolved from prediction based on a few tree-ring chronologies (e.g., Axelson et al., 2009) to the use of tree-ring data from a relatively large network of sites as demonstrated here. Each stand of old trees preserves a unique record of environmental variability. Therefore, data from more sites captures more components of the seasonal and interannual variation in hydroclimate. We took further advantage of the density of our tree-ring network by generating ensembles of tree-ring reconstructions of water-year flow, which enabled a dynamic representation of uncertainty. Sauchyn et al. (2015a, 2015b) developed a recursive algorithm to generate large ensembles of statistically significant reconstructions. The number of potential models is extremely large: "$N!/(N - n)!$" permutations of "n" predictors from the pool of "N" tree-ring chronologies; in our case, $n = 5$–9 and $N = 196$. The

algorithm repeats the forward selection process, beginning with the single model found by conventional forward selection, recursively removing predictors from the available pool, while retaining all models that exceed a threshold R^2_{adj} above which the models are statistically significant ($p < 0.05$). The algorithm simultaneously proceeds along all "*n*" branches at each level (row) resulting in, more or less, uniform decline in model quality. Run to completion, the script would evaluate every subset of "*n*" predictors (a best-subsets analysis), but is more likely to find better models earlier in the process. When stopped at an arbitrary point, the script stores, in descending order by R^2_{adj}, the output and validation statistics for an ensemble of statistically significant models. We determined that an ensemble of 100 reconstructions captured the statistical distribution of proxy flows of larger ensembles. Therefore, for each nest, we retained the water-year flows generated by the 100 models with the highest R^2_{adj}. The 100 models per nested ensemble each consist of a unique combination of predictor tree-ring chronologies identified in Table S4 in the supporting information.

Hypothetically, the availability of subannual tree-ring data from a large network of sites should capture more of the seasonal and spatial variability in watershed hydrology than annual ring-width data from a few sites, such as those that were the basis of the previous reconstructions of the flow of the SSR and NSR (Axelson et al., 2009; Case & Macdonald 2003; Sauchyn et al., 2011). Much improved model statistics supports this hypothesis. Supporting information Table S3 provides, for each nested ensemble of 100 tree-ring models of water-year flow, the number of potential and model predictors, and the median and range of calibration and validation statistics. These statistics indicate robust models with considerable predictive power. Typical reconstructions river flow are based on tree-ring models that account for about 50% of the variance in the predictand. In this study, we achieved R^2_{adj} values in the range of 50–80% for the reconstruction of flow back to the early 1500s and R^2_{adj} of 40–50% for the preceding four centuries. The full tree-ring reconstructions are plotted in Figure 3 as departures from the mean water-year flow in each basin. In this format, the historical low flows, during the 1930s, 1980s, and early 2000s, are clearly visible. More notable, however, are the periods of low flow that exceed the historical worst-case scenario in term of both severity and duration. The decadal scale of hydroclimate variability is also evident in these plots in terms of successive years of high and lows flows lasting one to three decades. Notable periods of low flow are the prolonged "megadroughts" of the 14th century (NSR) and 1470–1570 (SSR), and the intense droughts of the 18th century, which have been related to regional sand dune activity (Wolfe et al., 2001).

The plots in Figure 4 are ensemble reconstructions for the two rivers. They illustrate that many similar and valid paleohydrological records can be derived from a large pool of tree-ring proxies. The range of inferred values in the full ensemble provides an indication of the degree of time varying uncertainty. There is good agreement among the 100 reconstructions since about 1300 in the SSRB and 1400 in the NSRB. Prior to that more discrepancy and larger uncertainty reflect decreasing sample depth.

A conventional approach would dictate that we would base a streamflow reconstruction on output from the best single model (highest R^2_{adj} and RE; lowest SE and RMSEv), but this study again departed from standard practice by using instead the mean of the ensemble shown as the red curves in Figure 4. Use of the ensemble mean as the preferred proxy record was prompted by our initial analysis of the stochastic flows generated from single models. Figure 4 illustrates that single models generate some extremes values, such as SSR flows that approach zero. These extreme values in the tree-ring record could not be reproduced by stochastically deriving 10,000 annual flow series from the ~100 year gauge record, using the procedures described in the next section of this paper. That is, these extreme proxy flows had a very small probability of exceedence (<0.001). Whereas a 900 year time series could conceivably include water levels that are well outside the range of historical flows, these extreme values could also reflect a nonlinear response of radial tree growth to fluctuations in soil moisture (Cook & Pederson, 2011). There is a more or less linear relationship between standardized tree-ring width and hydroclimate with the exception of extremes of the soil water balance. The observation of anomalously wide annual tree rings suggests that the moisture limitation on tree growth at dry sites is lifted in unusually wet years. Conversely, tree rings that are missing, or have the width of a single cell, indicate a physiological response of trees to extreme local aridity. While these tree rings undoubtedly correspond to years of drought, the runoff over a large watershed very likely was greater than implied by these missing or anomalously narrow tree rings from a site chronology that otherwise correlates with streamflow. The mean value of a 100 member ensemble captures these extremely wet and dry years, while suppressing the influence of anomalously large or narrow ring-width index values on the reconstruction of streamflow.

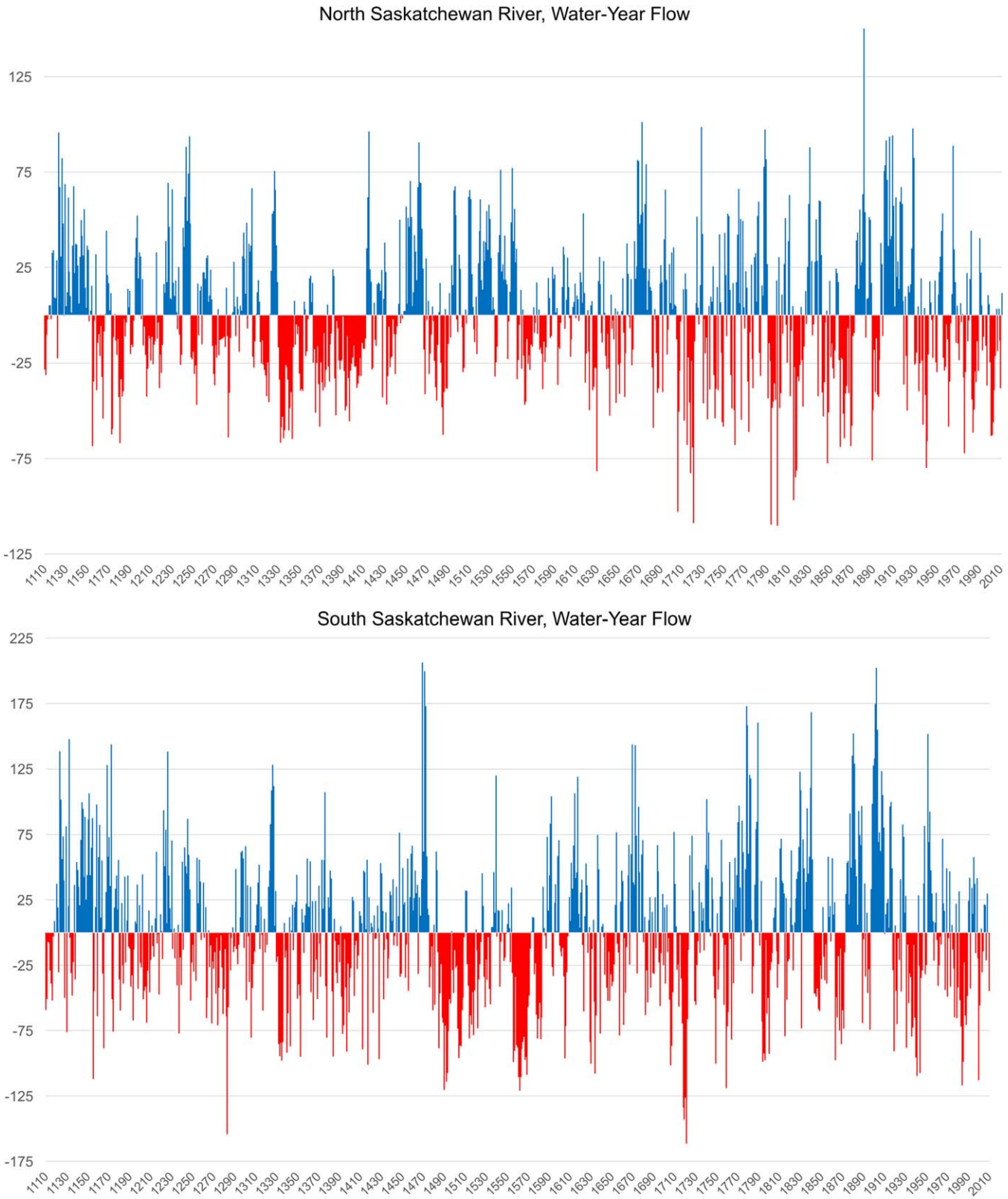

Figure 3. The full tree-ring reconstructions of water-year flow plotted as positive (blue) and negative (red) departures from the mean water-year flow in each basin.

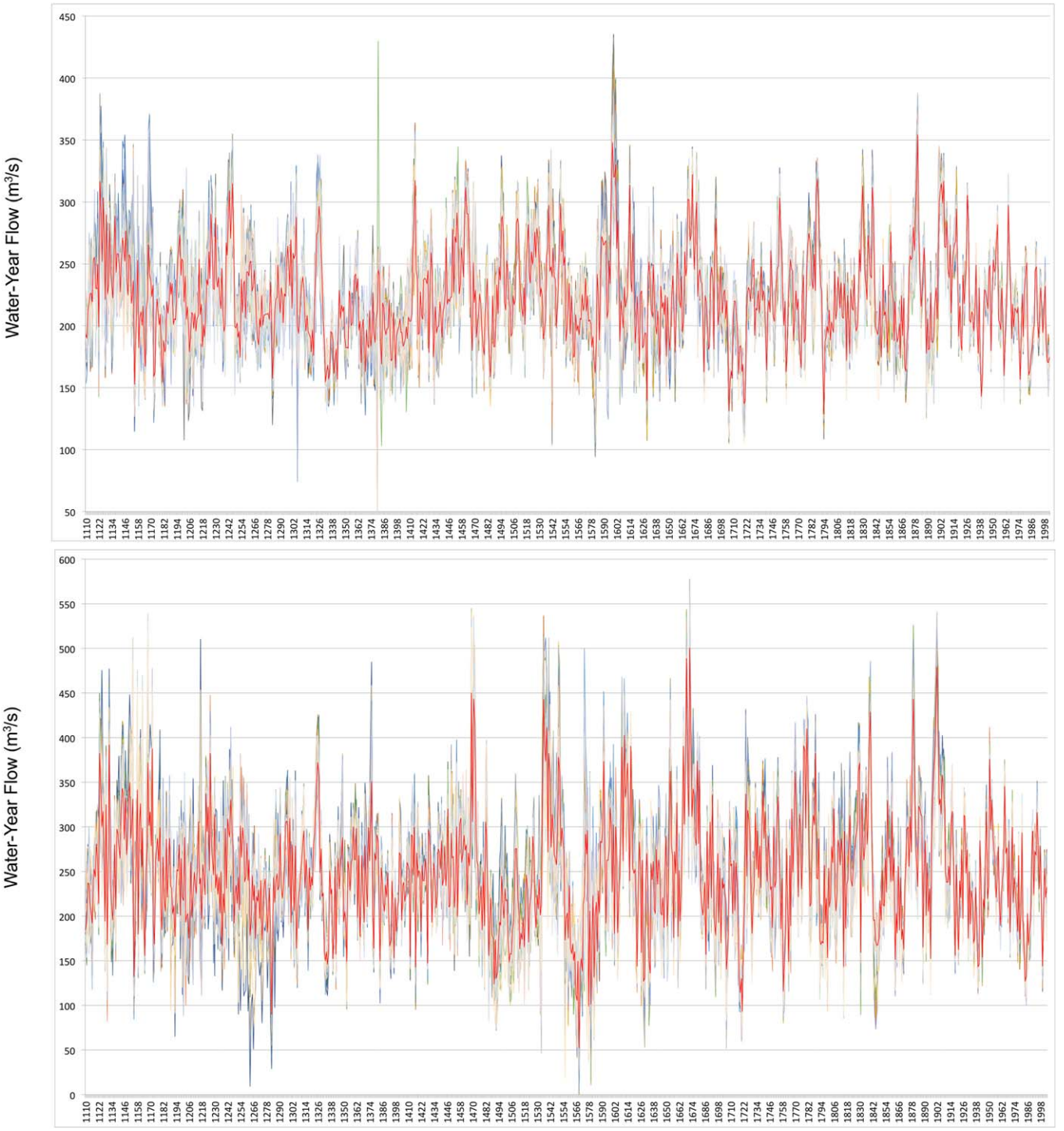

Figure 4. Ensembles of 100 reconstructions of the water-year flow of the NSR and SSR with the mean reconstruction plotted in red.

4. The Stochastic Estimates of Weekly Flows

The ultimate stage in the process of generating 900 years of weekly streamflows was developing an algorithm to stochastically downscale the mean of an ensemble of annual streamflow reconstructions. The algorithm ensures that the weekly time series have the statistical characteristics of both the naturalized recorded flows and the paleohydrology. The range and sequence of flows is constrained by both the historical seasonal cycle and the lower-frequency interannual to decadal variability in the tree-ring data.

The established statistical inference between tree-ring width and historical annual flows is the basis for creating the estimates of the annual flows for all years of data available from the tree rings. Although they contain important information about the length and severity of dry years, at an annual scale, the inferred flow volumes are of limited use in river basin management, and they should be disaggregated into weekly flows. Classical disaggregation techniques originally proposed by Valencia and Schaake (1973) are considered outdated due to their inability to preserve multiple statistical dependencies among weekly flows at multiple sites for higher order lags. More recent nonparametric techniques proposed by Tarboton et al. (1998) have the potential to overcome this limitation. The algorithm applied in this study relies on the previous work of Ilich (2009, 2013). While this algorithm was not originally designed for decomposition of annual flows, it required only minor adjustments to accommodate this process, as is briefly explained in the following.

Consider a problem of generating n random variables with arbitrary distribution functions and with a given correlation structure. Both the distribution function and the correlation structure can be obtained from the available historical data. In hydrology, we could assume that each of the 52 weekly flows is an independent statistical variable with its own distribution function. Also, each weekly flow is correlated to the flows in previous weeks according to the correlation matrix coefficients. This is depicted graphically in Table 1, which shows weekly flows arranged in a matrix format, along with the accompanying correlation matrix that was calculated on the basis of the m years of the available historical flow data.

This algorithm relies on its ability to create any number of synthetic years with weekly flows that will maintain both the probability of the distribution function for each week, as well as the correlation structure defined by the correlation matrix among the 52 weeks. This is equivalent to solving a problem of generating n random variables with arbitrary statistical distribution functions and a given correlation structure. Such algorithms already exist. Iman and Conover (1982) proposed the first one. Many similar developments followed, with recent algorithms that are more flexible and accurate (Ilich, 2009). The advantage of applying this approach in hydrology is obvious, since preservation of the correlation structure for all 52 weeks automatically addresses statistical dependence of generated flows for all significant lags between week 1 and week 52. In general, these algorithms have two steps:

1. Generate a desired number of realizations of each variable (in this case weekly flows) using the statistical distribution function selected to represent those variables; and,
2. Reorder (or permute) flows generated for each week in step (1) such that the desired correlation structure is induced, i.e., the reordered generated flows give a correlation matrix that closely resembles the correlation matrix of historical flows.

Table 1
Matrix Representation of Historical Weekly Flows

	Station 1 Weeks						
Year	1	2	3	.	.	51	52
1	$X_{1,1}$	$X_{1,2}$	$X_{1,3}$	.	.	$X_{1,51}$	$X_{1,52}$
2	$X_{2,1}$	$X_{2,2}$	$X_{2,3}$	.	.	$X_{2,51}$	$X_{2,52}$
3	.						
.	.	.	.	.	.	.	.
$m-1$	.						
m	$X_{m,1}$	$X_{m,2}$	$X_{m,3}$	.	.	$X_{m,51}$	$X_{m,52}$
Correlation matrix							
Variable							
1	1	$\sigma_{1,2}$	$\sigma_{1,3}$	.	.	$\sigma_{1,52}$	$\sigma_{1,52}$
2		1	$\sigma_{2,3}$	.	.	$\sigma_{2,52}$	$\sigma_{2,52}$
3			1				
.					.	.	.
$n-1$						1	
n							1

These steps are explained in detail in the referenced literature (Ilich, 2009, 2013); only a brief outline is provided in the following.

Step 1. Random generation of weekly flows. This step does not view weekly flows as time series, but rather as independent random variables for each individual week that have their own distribution functions. Two approaches can be used to independently generate flows for each week, and those are by:

1. Fitting a typical statistical distribution to the flow data for a particular week, or
2. Using the historical data to define an empirical distribution.

Figure 5 provides an example of these two approaches for the Bow River at Calgary in week 20. There were 90 years of weekly data, hence there are 90 empirical points shown in Figure 5.

An Extreme Value (EV) distribution fit is presented in Figure 5 using the cumulative distribution function. The data fit for both the empirical and theoretical functions in Figure 5 is good, however, this may not always be the case when theoretical distributions are used, while it is virtually guaranteed with empirical distributions within the available data range. Hence, instead of fitting different functions for each week and going through various goodness of fit tests, it is possible to

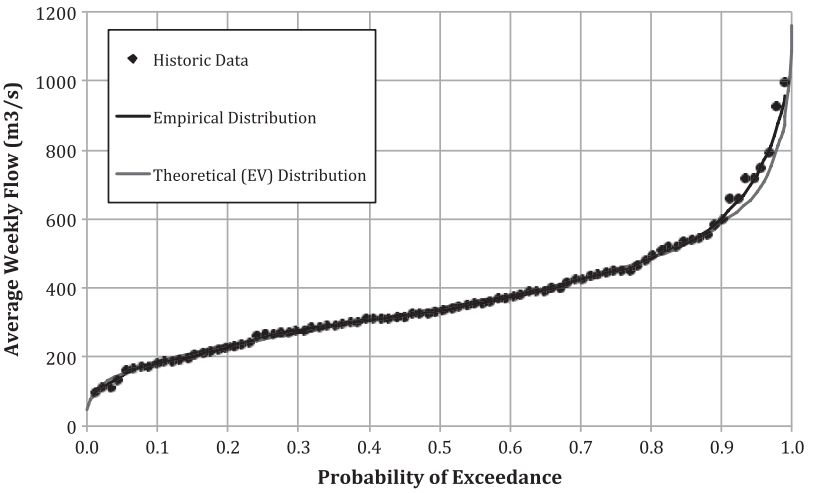

Figure 5. Empirical and theoretical distributions of weekly flows.

use empirical distributions, such as, for example, a Kernel density function. Sharma et al. (1997) define Kernel density estimation as a function that "entails a weighted moving average of the empirical distribution of the data". The popular Gaussian Kernel was used here, with the standard bandwidth of $h = 1.06\sigma n^{-1/5}$ selected for the univariate case as originally defined by Silverman (1986, pp. 86–87), with σ being the standard deviation of the data sample of size n. While this removes the need to fit theoretical distributions to the data within the available data range, there is still the issue of fitting the function at the tail ends of the statistical curves where empirical data are not available. Moon et al. (1993) gave an extensive report on the comparison of probability estimators for tail ends statistical functions used in hydrology, which is also summarized by Lall (1995) in a comprehensive review paper on the use of non-parametric functions in hydrology. While there are ways to rely on the Kernel estimates beyond the range of the available data, Moon et al. (1993) tested an entire class of methods that assumed a "parametric form for the tail, but not for the entire probability model." Their conclusions are that this approach gives acceptable models, and that there was no clear winner in terms of the selection of the theoretical model. Typical functions tested for the tail ends are those that are well known to fit rare events in hydrology, including the extreme value (EV) distribution that was selected in this study and fitted to a subset of weekly flows for each individual week independently by using the method of moments, with EV type I (Gumbel) being used for high flows and EV type III being used for low flows, as detailed by Moon et al. in their 1993 paper.

When a sufficient number of points (i.e., close to 100 years of data) are available on the empirical curve, adding theoretical extensions is a relatively straight forward process, as can be seen in Figure 5. If the empirical and theoretical curve have an intersection point close to the last data point in the empirical curve, then the theoretical curve is used from the interception point, to cover the probabilities that are beyond the data range and therefore cannot be assessed using any of the plotting position formulas. This case can be observed on the low flow end of the statistical curve in Figure 5. The other possibility is that the two curves do not have an intersection point at the tail end of the empirical curve, as is the case with the high flow range in Figure 5. In that case, the empirical curve is extrapolated by numerically evaluating its gradient in the final section of the curve, and the short extrapolated segment is used to find the intersection point with the theoretical curve. Any probabilities beyond the intersection point are then read from the theoretical curve. This process is automated using numerical assessment of the gradient of the empirical curve. It ensures smooth transition from empirical to theoretical segments of the probability distribution function.

Having established a way to develop a statistical distribution function for every week, we can generate any number (e.g., 10,000) of realizations of weekly flows for each week. At the end of Step 1, weekly flows will conform to the statistical function, but they will be mutually independent of each other, which implies correlation coefficients close to zero among all weeks.

In Step 2, the weekly flows generated in Step (1) are permuted inducing the desired correlation among all weeks within each year. In other words, flows generated in Step (1) are permuted in such a way that their

correlation matrix closely resembles the correlation matrix of the original historical data. This can be done using the algorithm originally proposed by Iman and Conover (1982), or by using more recent algorithms developed for this purpose (Ilich, 2009). These algorithms have been dealt with in sufficient detail in the literature such that their explanation need not be repeated here.

At the end of Step (2), 10,000 (or more) years of generated weekly flows have the desired weekly distribution functions and mutual correlation structure among weeks within each year. We have also generated 900 years of annual flow data based on the tree-ring proxy. The algorithm can now proceed to its final step, in which 900 years of generated weekly flows will be selected from the pool of 10,000 generated years of data such that two criteria are met simultaneously:

1. the mean annual flow of the selected years with be very close to the mean annual flows established from the tree-ring proxy; and,
2. the correlation structure of the weekly flows that cross from year i to year $i + 1$ will be similar to the one found in the historical weekly flow data.

To enable this process, we need a sufficiently large pool of weekly data. By applying this algorithm to various river basins, using simulations with up to 200,000 hypothetical years, we determined that 10,000 generated years is a sufficiently large pool to select a roughly 10 times smaller subset.

Step 3 is the final selection of the appropriate years of weekly flow series. The criteria for selection of suitable years of weekly flows from a pool of 10,000 years are associated with minimizing the weighted sum of deviations from the target annual mean flow defined in the tree-ring series and the sum of squares of differences between the historical and simulated weekly correlations for the transitional weeks from year to year. Typically, a threshold is established for correlation significance (e.g., r = 0.4 or 0.5), which determines the number of weeks that should be taken into account. In practical terms, for most basins there is no need to consider more than four weeks at the end of year *i* and 4 weeks at the beginning of year $i + 1$. The goal is to minimize the sum of deviations from the two targets:

$$\min Ck = Ra + Dk$$

where *Ra* is the relative error of the annual flow of the year selected from the 10,000 weekly flow pool with respect to its annual flow target defined by any given year in the tree-ring series, while *Dk* is the sum of squares of distances for the significant correlations among weekly flows that cross from year to year, defined using the following expression:

$$Dk = \sum_{p=1}^{L} \sum_{q=n-L+p}^{n} (\rho_{q,p}^{k} - \sigma_{q,p}^{k})^2$$

where *L* is the significant lag expressed in the number of weeks (typically 4 or less), $\rho_{q,p}$ and $\sigma_{q,p}$ are the respective correlations between weeks *q* and *p* of the historical and simulated weekly data, *n* is the total

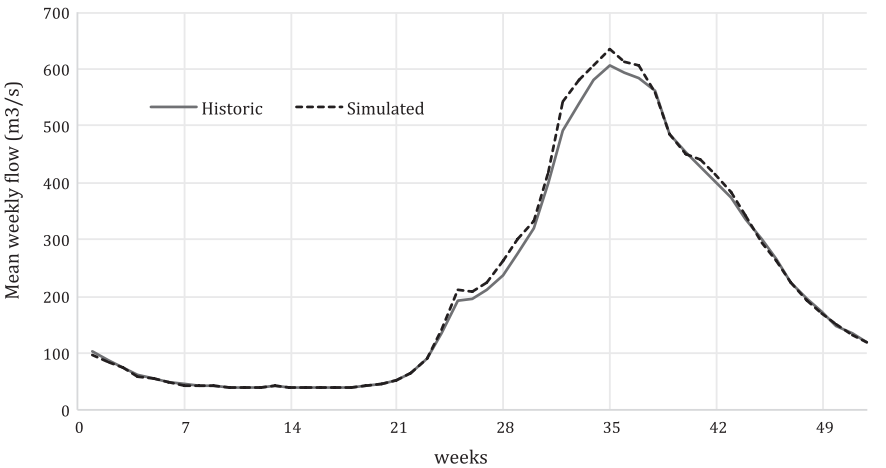

Figure 6. Comparison of the historical and simulated mean weekly flows.

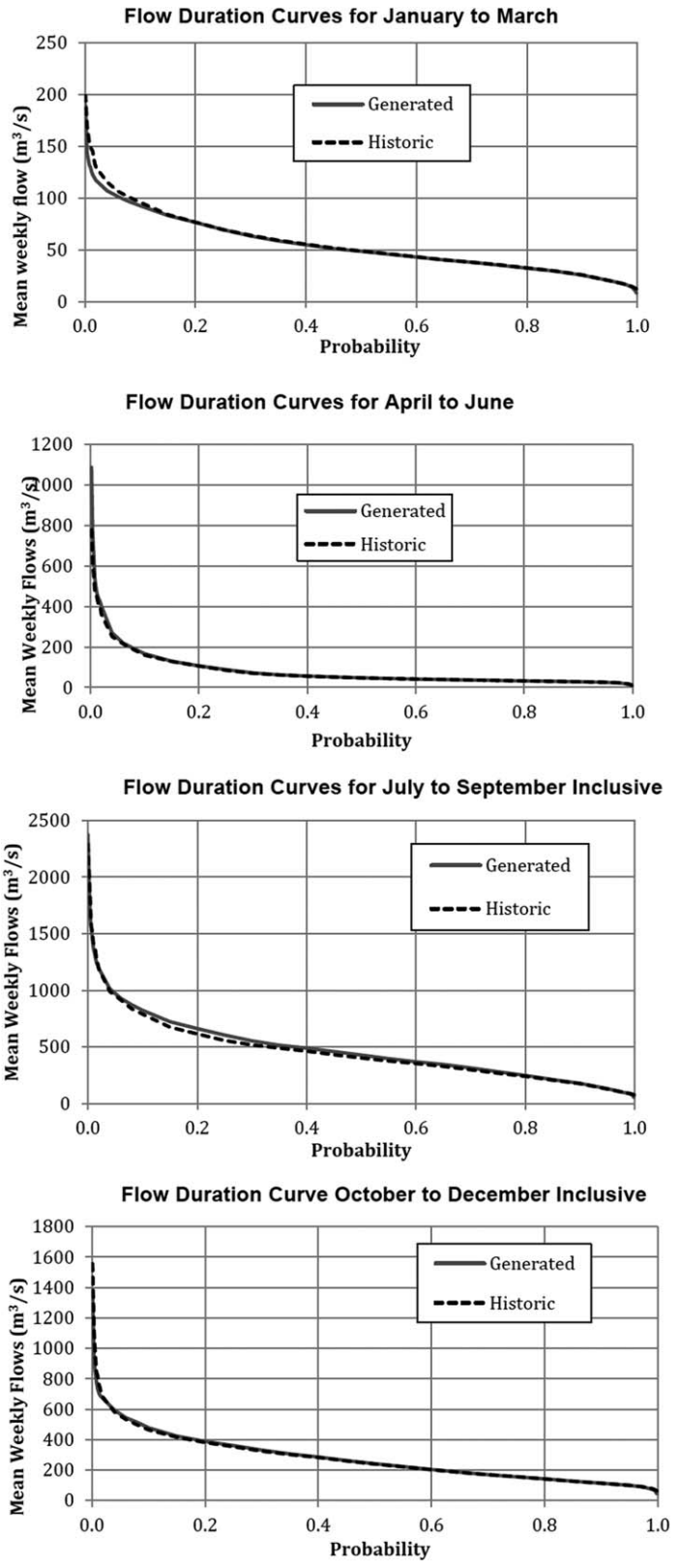

Figure 7. Quarterly historical and simulated flow duration curves.

number of weeks (52) and *k* is the year index for which the statistic is calculated. Essentially, the algorithm is looking for a year that has a desirable annual flow (calculated by averaging all weekly flows for a selected year) and a desirable statistical dependence between the first 4 weeks of flows and the last 4 weeks of flows of the previous year.

The algorithm uses a direct search through several simple steps to achieve its goal:

1. The first step is to sort all 10,000 years of generated weekly flows on the basis of the value of mean weekly flow for a year;
2. The next step is to select the first year of the tree-ring series and find the best match for it in the sorted series of simulated flows. For the first year, this is sufficient. The selected year is then removed from the pool of 10,000 years. For all subsequent years, the *Dk* statistic is calculated for the best match and the algorithm proceeds to the next step.
3. The algorithm then moves away from the best match and calculates the composite statistic *Ck* for all years that have a difference from the target annual flow of less than 1%.
4. All calculated statistics *Ck* are then compared and the one with the lowest value is selected. The corresponding year is then removed from the pool of 10,000 years with weekly flow data, and the algorithm proceeds in the same way until all years have been selected.

The above procedure is straightforward. The user has an option to generate any number of simulated years. Simulations with up to 200,000 hypothetical years of weekly years were generated, but the results were not considerably better than the typical 10,000 years that were sufficiently good, while the execution times were considerably shorter. The model runs as a web application available at www.optimal-solutions-ltd.com. This application requires only the annual flows based on the tree-ring series and weekly flows in a matrix format, both of which are uploaded using the copy and paste function, while the results are delivered as a downloadable zipped file in ASCII format. The process is simple and there is a short user's manual available on the web site. This web application is described in more detail in the supporting information file.

5. Verification of Simulated Weekly Flows

The proposed model is considered successful if it meets all its stated goals, namely if (a) the mean annual flows from the selected weekly series compare well with the desirable annual flow targets dictated by the tree-ring series; (b) the weekly statistical distribution functions of the generated series are similar to the historical; and (c) the correlation structure of the simulated weekly series is similar to the historical series.

Weekly means and quarterly statistical distribution functions for simulated and historical North Saskatchewan River data are shown in Figures 6 and 7. The Weibull plotting position formula was used to generate the plots, although in the presence of large amount of data the plots would not look different with any other plotting position formula.

Statistical dependence is verified by comparing correlation coefficients of weekly flows for the historical and simulated series. Of

Table 2
Historical and Simulated Correlation Coefficients for Transitional (Year to Year) Weeks

Historical	Week 49	Week 50	Week 51	Week 52	Week 1 ($i+1$)	Week 2 ($i+1$)	Week 3 ($i+3$)	Week 4 ($i+4$)
Historical								
week 49	1.00							
Week 50	0.93	1.00						
Week 51	0.87	0.94	1.00					
Week 52	0.76	0.81	0.90	1.00				
Week 1 ($i+1$)	0.75	0.79	0.86	0.91	1.00			
Week 2 ($i+1$)	0.63	0.68	0.74	0.75	0.84	1.00		
Week 3 ($i+3$)	0.48	0.54	0.56	0.53	0.58	0.71	1.00	
Week 4 ($i+4$)	0.54	0.59	0.60	0.57	0.60	0.64	0.75	1.00
Simulated								
Week 49	1.00							
Week 50	0.88	1.00						
Week 51	0.80	0.92	1.00					
Week 52	0.66	0.76	0.87	1.00				
Week 1 ($i+1$)	0.68	0.79	0.86	0.91	1.00			
Week 2 ($I+1$)	0.59	0.68	0.74	0.75	0.78	1.00		
Week 3 ($I+3$)	0.46	0.54	0.57	0.54	0.56	0.68	1.00	
Week 4 ($I+4$)	0.36	0.44	0.46	0.45	0.47	0.50	0.65	1.00

particular interest are the correlation coefficients between the last 4 weeks of year *i* and the next 4 weeks of the subsequent year *i + 1*. They are presented in Table 2.

The correlation matrix is symmetrical, so it is sufficient to show only values in the lower triangular or the upper triangular matrix. Historical correlation between week 52 of any given year and week 1 of the subsequent year is 0.91, and this value is the same in the simulated series. Table 2 shows that the simulated and historical series exhibit a similar pattern of statistical dependence among the weekly flows. Autocorrelation functions of lag-1 and lag-2 are typically assessed for time series after removing seasonality. However, autocorrelation may change with the seasons of the year, and those changes should also be preserved in the simulated series. Table 3 gives the autocorrelation of lag-1 and lag-2 for both historical and simulated series, averaged over 4 week periods. Similar values in the historical and simulated series in Tables 2 and 3 demonstrate that the algorithm is able to deliver weekly hydrologic series with the desired correlation structure.

The outcome of the model is a series of 900 years (in this case) of generated weekly flows that are in agreement with the annual flows obtained from tree rings while all relevant weekly statistics are preserved. In Figure 8 the tree-ring inferred water-year flows are plotted along with the weekly flow estimates summed by water year. As dictated by the stochastic flow generator, the weekly flows sum to match the reconstructed water-year flow. When we originally plotted the summed stochastic weekly flows and output from a single model of water-year streamflow (not shown), there were discrepancies in years of extreme low flow. This led to our conclusion that extreme growing-season aridity at individual sites can produce anomalous tree rings that are not representative of the annual runoff from a large watershed. Therefore, we used the ensemble means, with outliers that are statistically plausible low flows according to a probably distribution which fits the historical record and is well suited for rare hydrologic events.

Table 3
Historical and Simulated Autocorrelations of lag-1 and lag-2 for 4 Week Periods

4 week period	AC-1 historic	AC-1 simulated	AC-2 historic	AC-2 simulated
1	0.75	0.68	0.52	0.42
2	0.69	0.62	0.50	0.38
3	0.70	0.65	0.53	0.47
4	0.79	0.77	0.61	0.58
5	0.70	0.69	0.47	0.46
6	0.50	0.49	0.20	0.19
7	0.65	0.70	0.35	0.40
8	0.68	0.64	0.38	0.31
9	0.60	0.50	0.46	0.29
10	0.66	0.53	0.50	0.32
11	0.70	0.62	0.50	0.37
12	0.85	0.80	0.73	0.63
13	0.92	0.89	0.82	0.79

6. Discussion

The research described in this paper resulted in a unique hydrometric data set: 900 years of weekly flow estimates for the South and North Saskatchewan Rivers reconstructed from tree-rings and scaled to weekly resolution using methods of stochastic hydrology. Expanding the hydrometric record, from 100 to 900 years, results in more extreme weekly flows in the tails of the probability distribution. The

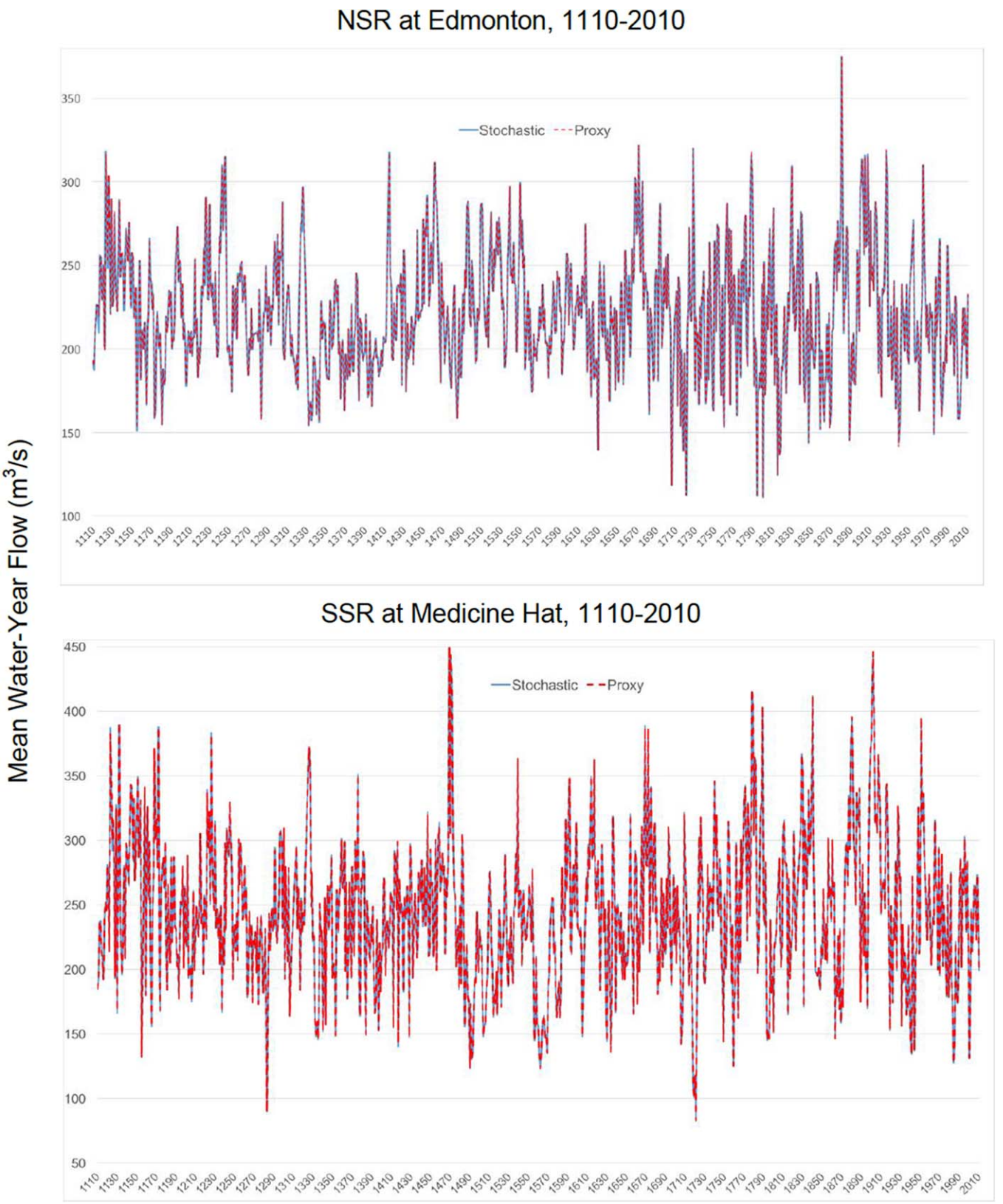

Figure 8. Time series of tree-ring inferred (red) and summed weekly stochastic flows (blue). The tree-ring reconstructions are the ensemble means from Figure 4.

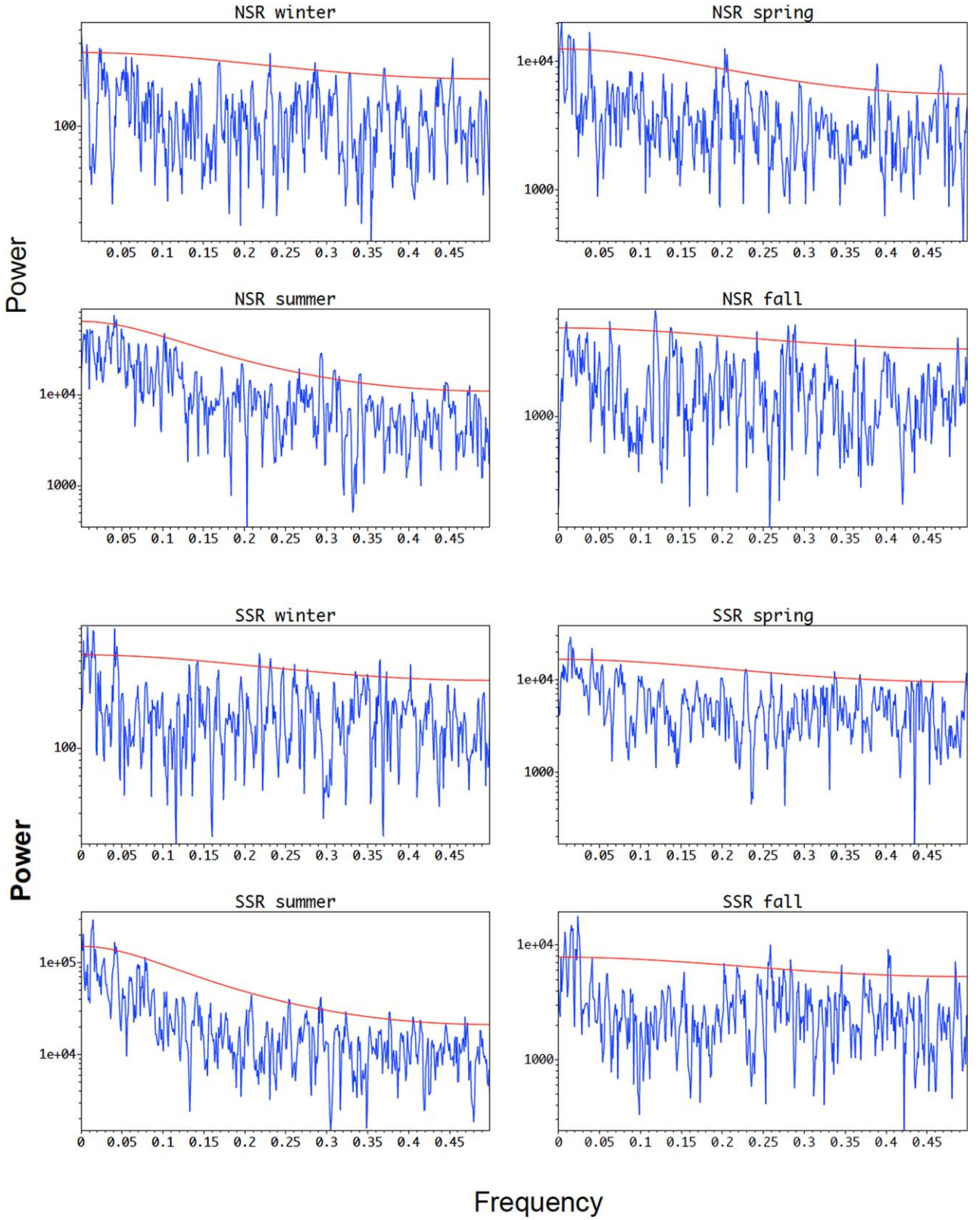

Figure 9. Multitaper method (MTM) spectral analysis of the mean seasonal flows of South and North Saskatchewan Rivers (NSR, SSR) over the period of the tree-ring reconstruction, 1110–2010.

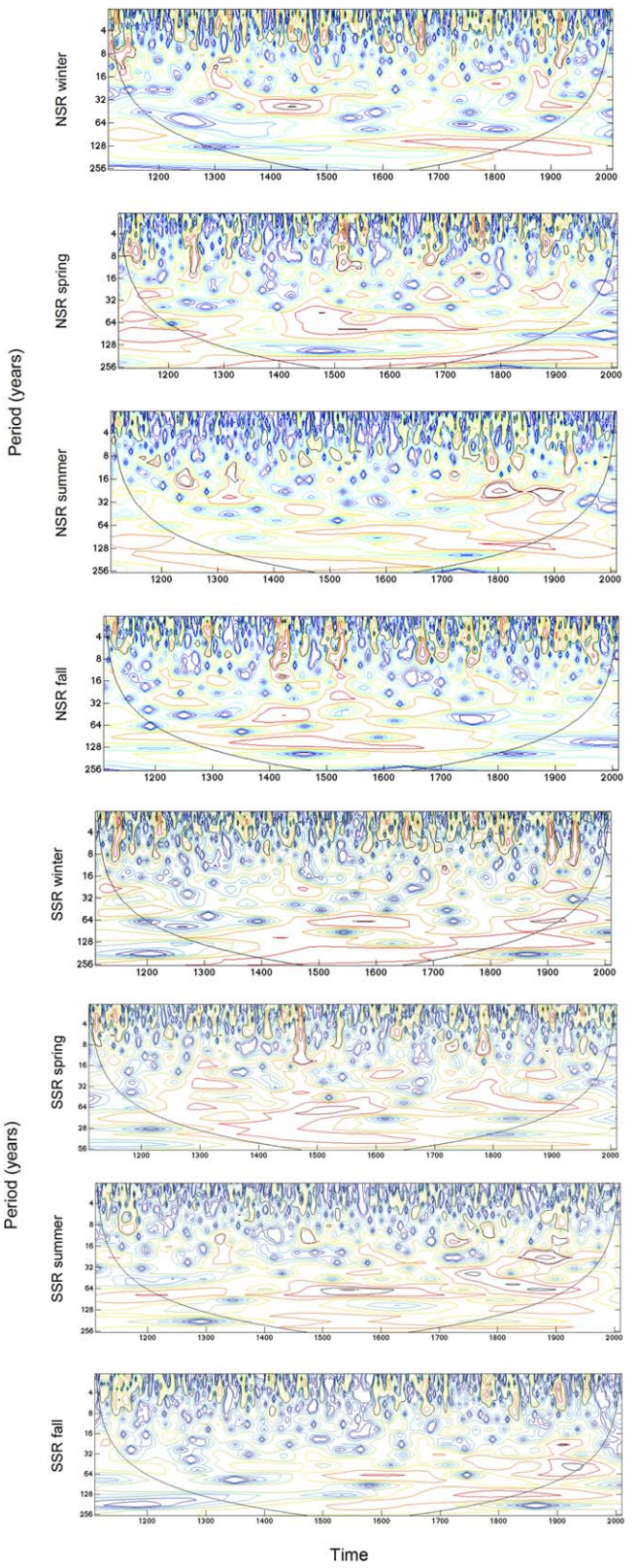

Figure 10. Wavelet transform plots of periodic variability in the mean seasonal flow of the North and South Saskatchewan Rivers (NSR, SSR) over the period of the tree-ring reconstruction, 1110–2010. The red isolines, within the cone of influence, represent statistically significant ($p < 0.05$) spectral power.

long high-resolution paleoflow series includes years and periods of low flow of greater severity and duration than the droughts of record in the much shorter historical time frame. Preinstrumental droughts were one to two decades in duration and included years when the stream flow deficit exceeded the minimum annual flows in the gauged record.

Various methods have been proposed to capture the variability and uncertainty in tree-ring reconstructions of streamflow. Our method of characterizing uncertainty has two stages. First, we take an innovative approach to characterizing the dynamic uncertainty in the tree-ring reconstructions of annual river flows by generating an ensemble of 100 reconstructions for each gauge. Second, stochastic temporal disaggregation of the ensemble mean captures the uncertainty in the weekly flow estimates. We compare the distributions and statistical properties between these simulated weekly flows and the historical gauge data. We were able to demonstrate our confidence in the inference of stream flow from tree rings by generating the 100 reconstructions for each gauge, displaying the range of proxy flows captured by these ensembles. This approach took advantage of the density of our tree-ring network and the availability of 196 potential tree-ring predictors of river flow. There are precedents for this approach; Woodhouse and Lukas (2006) produced an ensemble of 10 reconstructions. Among alternative methods, the K-NN based approach of Gangopadhyay et al. (2009) also generates ensembles of streamflow reconstructions and a dynamic representation of uncertainly. However, the Gangopadhyay et al. method uses combinations of observed streamflows to construct modern analogues of reconstructed streamflow series. This approach limits the long-term variability in the streamflow reconstruction to the range of recorded flows, whereas our method is not subject to this limitation.

By extending streamflow time series from decades to centuries, and even millennia, dendrohydrology enables the analysis of periodic variability at frequencies that approach the length of gauged records, and the analysis of higher frequency modes of variability with greater sample depth. Given our 900 years of weekly proxy flow estimates for the SRB, we are able to downscale the analysis of hydroclimatic variability to the seasonal scale. Figure 9 gives the results of multitaper method (MTM) spectral analysis of seasonal flows computed by averaging the flow estimates for the 13 weeks in each season over the full period of the tree-ring reconstruction (1110–2010). A wavelet transform of the seasonal streamflow (Figure 10) shows this periodic variability in the time domain. These plots demonstrate that the stochastic paleohydrology exhibits the dominant modes of variability characteristic of the hydroclimate of western North America. The frequencies with statistically significant ($p < 0.05$) power (spectral density) are in the range of 0.2–0.5 (2–5 years) and 0.04/0.02–0.015 (25/50–70 years). These frequencies correspond to commonly cited periodicities of the high frequency El Niño Southern Oscillation and lower-frequency Pacific Decadal Oscillation and their strong teleconnections to the regional hydroclimate (Ault et al., 2013; Sauchyn et al, 2017). The wavelet plots (Figure 10) illustrate the nonstationarity of these modes of variability, with a tendency for more power at lower frequencies in the past two centuries and the midmillennium.

The results achieved here are transferable to other river basins, with application to drought mitigation, reservoir operation, design of hydraulic structures, analyzing the performance of rural water management systems, assessing climate change impacts, reconstructing flows in ungauged watersheds, and developing long-term watershed protection plans. There are policy implications for water allocation and apportionment, regional land use planning, water conservation and source water protection, water conveyance and storage, and drought preparedness and mitigation strategies. The novel scientific methods employed here have produced a rich database of hydroclimatic data with potentially various applications to watershed and water resource management. These applications are beyond the scope of the current study, but might include:

1. From probability density functions and flow duration curves, establishing the probability of exceeding critical water levels specific to a river basin. Water allocation and surface water management usually are based on sub-annual flow data, such as seasonal or weekly flow triggers and cumulative water withdrawal limits. The critical flows that trigger seasonal water use restrictions, as specified by the City of Calgary (2011), are a good example.
2. Characterizing an extended drought in terms of the timing and sequence of weekly flows, and determining the probability of consecutive low/high flows, since prolonged and wet and dry conditions have significant cumulative impacts.
3. Testing of water management models and the evaluation of the reliability, resilience, and capacity of water supply and management systems when exposed to severe and prolonged low river levels.
4. Comparing climate model projections to the hydroclimatic variability captured by the 900 years of synthetic flows - do the climate models simulate the range of water levels and modes of variability found in the paleo/stochastic record?
5. Stochastic scaling of seasonal tree-ring reconstructions; we can further constrain the selection weekly flows from a randomized pool according to the seasonal paleohydrology as reconstructed from early-wood and late-wood density and width chronologies.

With the current and further global warming of the atmosphere and oceans, climate and water variables are trending away from historical values and extreme conditions are exceeding prior magnitudes and frequencies. Unprecedented water levels become increasingly probable over a long planning horizon, as required for the design and implementation of water conveyance, storage and treatment structures. Standard practice in water resources planning and engineering makes two key assumptions about historical data from water and climate gauges: that they (1) adequately represent the long-term trends and variability in climate and water variables, and (2) are stationary—that they fluctuate within a constant range of variability. Research on climate change brings into question these foundational assumptions in water resource engineering (Milly et al., 2008). Studies of past (preinstrumental) hydroclimate undermine the concept of stationarity by revealing extremes that are outside the range of historical observations and by demonstrating that climate and water regimes vary at decadal to multidecadal scales (Ault et al., 2013). Because these cycles exceed the length of most instrumental records, they generally are not considered for planning or practical purposes, and yet this scale of climatic variability has profound implications for the long-term feasibility of existing water management practices and structures.

Acknowledgments

This study was funded by Alberta Innovates, EPCOR Water Canada and the City of Calgary. For their support and collaboration, we thank Margaret Beeston (Leader, Resource Planning and Policy, Water Resources, The City of Calgary), Lily Ma (Team Lead, Resource Analysis, Strategic Services, Water Resources, The City of Calgary), Lyndon Gyurek (Senior Manager, Environment, EPCOR Water Canada) and Jon Sweetman (Manager, Water Resources, Alberta Innovates—Energy and Environment Solutions). The tree-ring data are archived with the International Tree Ring Data Bank (https://data.noaa.gov/dataset/international-tree-ring-data-bank-itrdb). Graduate students Iullia Andreichuk, Sunil Gurrapu, and Samantha Kerr assisted with the processing of data and preparation of the figures. Three anonymous reviewers provided substantive and insightful comments and constructive criticism. A sincere thank you to Brian Luckman, Professor Emeritus at Western University, for sharing tree-ring data from sites in Jasper and Waterton Lakes National Parks.

References

Ault, T. R., Cole, J. E., Overpeck, J. T., Pederson, G. T., St. George, S., Otto-Bliesner, B., . . . Deser, C. (2013). The continuum of hydroclimate variability in western North America during the last millennium. *Journal of Climate*, *26*(16), 5863–5878.

Axelson, J. N., Sauchyn, D. J., & Barichivich, J. (2009). New reconstructions of streamflow variability in the South Saskatchewan River Basin from a network of tree ring chronologies, Alberta, Canada. *Water Resources Research*, *45*, W09422. https:/doi.org/10.1029/2008WR007639

Case, R. A., & MacDonald, G. M. (2003). Tree ring reconstructions of streamflow for three Canadian prairie rivers. *Journal of the American Water Resources Association*, *39*, 703–716.

City of Calgary (2011). *Drought management plan* (53 pp.). City of Calgary, Alberta.

Cook, E. R., & Pederson, N. (2011). Uncertainty, emergence, and statistics in dendrochronology. In M. K. Hughes (Ed.), *Dendroclimatology, developments in paleoenvironmental research* (Vol. 11). Dordrech, the Netherlands: Springer. https:/doi.org/10.1007/978-1-4020-5725-0_4

Deser, C., Phillips, A. S., Alexander, M. A., & Smoliak, B. V. (2014). Projecting North American Climate over the next 50 years: Uncertainty due to internal variability. *Journal of Climate*, *27*, 2271–2296. https:/doi.org/10.1175/JCLI-D-13-00451.1

Durack, P. J., Wijffels, S., & Matear, R. J. (2012). Ocean salinities reveal strong global water cycle intensification during 1950 to 2000. *Science*, *336*, 455–458. https:/doi.org/10.1126/science.1212222

Elshorbagy, A., Wagener, T., Razavi, S., & Sauchyn, D. (2016). Correlation and causation in tree-ring-based reconstruction of paleohydrology in cold semiarid regions. *Water Resources Research*, *52*, 7053–7069. https:/doi.org/10.1002/2016WR018985

Gangopadhyay, S., Harding, B. L., Rajagopalan, B., Lukas, J. J., & Fulp, T. J. (2009). A nonparametric approach for paleohydrologic reconstruction of annual streamflow ensembles. *Water Resources Research*, *45*, W06417. https://doi.org/10.1029/2008WR007201

Government of Alberta (2010). *Fact about water in Alberta* (68 pp.). Edmonton: Government of Alberta.
Ilich, N. (2008). Shortcomings of linear programming in optimizing river basin allocation. *Water Resources Research*, *44*, W02426. https:/doi.org/10.1029/2007WR006192
Ilich, N. (2009). A matching algorithm for generation of correlated random variables with arbitrary distribution functions. *European Journal of Operational Research*, *192*(2), 468–478. https:/doi.org/10.1016/j.ejor.2007.09.024
Ilich, N. (2011). Improving real time reservoir operation based on combining demand hedging and simple storage management rules. *Journal of Hydroinformatics*, *13*(3), 533–544.
Ilich, N. (2014). An effective three-step algorithm for multi-site generation of stochastic weekly hydrological time series. *Hydrological Sciences Journal*, *59*(1), 85–98.
Ilich, N., & Despotovic, J. (2008). A simple method for effective multisite generation of stochastic hydrologic time series. *Journal of Stochastic Environmental Research and Risk Assessment*, *22*(2), 265–279. https:/doi.org/10.1007/s00476-007-0113-6
Ilich, N., Simonovic, S. P., & Amron, M. (2000). The benefits of computerized real-time river basin management in the Malahayu Reservoir System. *Canadian Journal of Civil Engineering*, *27*(1), 55–64.
Iman, R. L., & Conover, W. J. (1982). A distribution-free approach to inducing rank correlation among input variables. *Communications in Statistics - Simulation and Computation*, *11*(3), 311–334.
Kharin, V. V., Zwiers, F. W., Zhang, X., & Hegerl, G. C. (2007). Changes in temperature and precipitation extremes in the IPCC ensemble of global coupled model simulations. *Journal of Climate*, *20*, 1419–1444. https://doi.org/10.1175/JCLI4066.1
Knutti, R., & Sedláček, J. (2012). Robustness and uncertainties in the new CMIP5 climate model projections, *Nature Climate Change*, *3*, 369–373. https://doi.org/10.1038/Nclimate1716
Lall, U. (1995). Recent advances in nonparametric function estimation: Hydrologic applications. *Review of Geophysics*, *33*, 1093–1102.
Loaiciga, H. A., Haston, L., & Michaelsen, J. (1993). Dendrohydrology and long-term hydrologic phenomena. *Review of Geophysics*, *31*, 151–171.
Meko, D. M., & Baisan, C. H. (2001). Pilot study of latewood-width of conifers as an indicator of variability of summer rainfall. *International Journal of Climatology*, *21*, 697–708.
Meko, D. M., Touchan, R., Díaz, J. V., Griffin, D., Woodhouse, C. A., Castro, C. L., . . . Leavitt, S. W. (2013). Sierra San Pedro Mártir, Baja California, cool-season precipitation reconstructed from earlywood width of abies concolor tree rings. *Journal of Geophysical Research: Biogeosciences*, *118*, 1660–1673. https://doi.org/10.1002/2013JG002408
Meko, D. M., & Woodhouse, C. A. (2011). Dendroclimatology, dendrohydrology, and water resources management. In M. K. Hughes, T. W. Swetnam, & H. F. Diaz (Eds.), *Tree rings and climate*. Dordrecht, Netherlands: Kluwer/Springer.
Meko, D. M., Woodhouse, C. A., & Morino, K. (2012). Dendrochronology and links to streamflow. *Journal of Hydrology*, *412–413*, 200–209. https://doi.org/10.1016.j.hydrol.2010.11.041
Milly, P. C. D., Betancourt, J., Falkenmark, M., Hirsch, R. M., Kundzewicz, Z. W., Lettenmaier, D. P., & Stouffer, R. J. (2008). Stationarity is dead: Whither water management? *Science*, *319*, 573–574.
Moon, Y., Lall, U., & Bosworth, K. (1993). A comparison of tail probability estimators for flood frequency analyses. *Journal of Hydrology*, *151*, 343–363.
Sauchyn, D. J., Bedoya, M., González-Reyes, Á., Muñoz, A., & Velez Upegui, J. J. (2017). ENSO signals and impacts along a semiarid to humid transect across the Americas. In *Proceedings of the 9th Biennial Rosenberg International Forum on Water Policy*. Los Angeles, CA: University of Southern California.
Sauchyn, D. J., Luckman, B. H., & St-Jacques, J.-M. (2015a). Long-term reliability of the Athabasca River (Alberta, Canada) as the water source for oil sands mining. *Proceedings of the National Academy of Science of the United States of America*, *112*(41), 12621–12626.
Sauchyn, D. J., Vanstone, J. R., St. Jacques, J.-M., & Sauchyn, R. D. (2015b). Dendrohydrology in Western Canada and applications to water resource management. *Journal of Hydrology*, *529*, 548–558.
Sauchyn, D. J., Vanstone, J. R., & Perez-Valdivia, C. (2011). Modes and forcing of hydroclimatic variability in the Upper North Saskatchewan River Basin Since 1063. *Canadian Water Resources Journal*, *36*, 205–218.
Sharma, A., Tarboton, D. G., & Lall, U. (1997). Streamflow simulation: An nonparametric approach. *Water Resources Research*, *33*, 291–308.
Silverman, B. W. (1986). *Density estimation for statistics and data analysis*. New York, NY: Chapman and Hall.
Tarboton, G. D., Sharma, A., & Lall, U. (1998). Disaggregation procedures for stochastic hydrology based on nonparametric density estimation. *Water Resources Research*, *34*, 107–119.
Valencia, D. R., & Schaake, J. L. Jr. (1973). Disaggregation processes in stochastic hydrology. *Water Resources Research*, *9*, 580–585.
Watson, E., & Luckman, B. H. (2005). Spatial patterns of pre-instrumental moisture variability in the southern Canadian Cordillera. *Journal of Climate*, *18*, 2847–2863. https://doi.org/10.1175/JCLI3416.1
Wolfe, S. A., Huntley, D. J., David, P. P., Ollerhead, J., Sauchyn, D. J., & Macdonald, G. M. (2001). Late 18th century drought-induced sand dune activity, Great Sand Hills, southwestern Saskatchewan. *Canadian Journal of Earth Sciences*, *38*(1), 105–117.
Woodhouse, C. A., & Lukas, J. J. (2006). Drought, tree rings and water resource management in Colorado. *Canadian Water Resources Journal*, *31*(4), 297–310.